Journal of Advanced Ceramics
2015, **4**(1): 22–30
DOI: 10.1007/s40145-015-0127-3

ISSN 2226-4108
CN 10-1154/TQ

Research Article

Synthesis, characterization and sintering behavior influencing mechanical, thermal and physical properties of pure cordierite and cordierite–ceria

Marikkannan SENTHIL KUMAR[a,*], Ayyasamy ELAYA PERUMAL[b], T. R. VIJAYARAM[a]

[a]*School of Mechanical Building and Sciences, VIT University, Chennai-600 127, Tamil Nadu State, India*
[b]*Department of Mechanical Engineering, Anna University, Chennai-600 025, Tamil Nadu State, India*

Received: May 26, 2014; Revised: August 27, 2014; Accepted: September 10, 2014

Abstract: The study of cordierite ceramic is the need of the hour in present technological world for various advanced engineering applications. Cordierite, which has relatively poor mechanical properties, has induced the use of various dopants to study the improvement in mechanical properties. Thirst of seeking new materials with good mechanical properties has revived the research on ceria doped cordierite. Present research conducted on pure cordierite and ceria doped cordierite ceramics has investigated the results of characterization and studied their suitability. Pure cordierite and cordierite–ceria (CeO_2) composite ceramics synthesized for various stoichiometric composition (5–20 wt%) were compacted at 240 MPa and sintered between 600 ℃ and 1350 ℃ for 3 h. The characterization techniques used in this study were X-ray diffraction (XRD), thermogravimetric (TG) analysis and Fourier transform infrared (FTIR). The density was calculated using the Archimedes principle. Influence of the ceria addition on cordierite's mechanical properties such as hardness, flexural strength and fracture toughness and on thermal properties as thermal expansion was studied. XRD results confirmed the presence of cordierite and ceria in the samples heat treated at 1350 ℃. Results of FTIR and TG analyses revealed the formation of cordierite and the effect of ceria addition. The mechanical properties studied were found to be encouraging and confirmed the suitability of cordierite–ceria as an alternate material for cordierite.

Keywords: cordierite; ceria (CeO_2); temperature; phase transformation; properties

1 Introduction

Since the discovery of cordierite by French geologist Cordier, it has been a subject of research till today. It is widely used in applications ranging from conventional to advanced engineering. Cordierite's properties include low dielectric constant, low coefficient of thermal expansion, high resistance to thermal shock and good mechanical properties [1]. These make cordierite ceramic an important material for study. Rankin and Mervin [2] studied on the phase diagram and reported the composition of cordierite as $MgO–Al_2O_3–SiO_2$. The stoichiometric composition of cordierite is $2MgO·2Al_2O_3·5SiO_2$ [3]. The availability of cordierite in its natural form is extremely rare and

* Corresponding author.
E-mail: msv305@yahoo.co.in, senthil.km@vit.ac.in

seldom occurs in commercial quantities. Therefore, cordierite is produced from synthetic origin. Many researchers have reported different techniques of cordierite fabrication such as co-precipitation, sol–gel and solid-state synthesis [4–8]. Cordierite fabricated using mixtures of clay (kaolin), talc and alumina or silica, and other raw materials as clay–feldspar–talc shows better electrical and thermal properties [9,10].

Cordierite which has a melting point of 1460 ℃ can be synthesized only at 1450 ℃. This presents narrow sintering range [11]. The polycrystalline cordierite ceramic of stoichiometric composition ($2MgO{\cdot}2Al_2O_3{\cdot}5SiO_2$) with high strength and density and low coefficient of thermal expansion (CTE) is very difficult to obtain due to its narrow sintering range and impurity-sensitive nature [12]. This shows that heating is very difficult at this sintering temperature without the sintering aid [13]. Cordierite can be synthesized at temperatures higher than 1300 ℃ [14]. Preparation of cordierite of high density and improved mechanical and thermal properties was attempted by addition of dopants like zirconia, ceria, titanium oxide, etc., using different techniques and with low sintering temperatures. Mullite addition into cordierite with different weight percentages (0–30 wt%) reported better densification behavior and mechanical properties of the composite [15].

The addition of zirconia into cordierite reported an increase in mechanical properties with low coefficient of thermal expansion. The mechanical properties were improved by transformation toughening. This has been demonstrated by different fabrication routes, such as conventional, precipitation, dispersion toughening and the sol–gel process, containing tetragonal (t) ZrO_2 particles [16–18]. Dispersion toughening of oxide ceramics by zirconia addition as a secondary phase is a well established process. It has been successfully employed to improve the mechanical properties by stress induced transformation toughening, micro-cracking and crack deflection [19]. In particular, cordierite system displayed enhanced mechanical properties by the addition of zirconia. It has shown many potential applications arising from its excellent thermal and dielectric properties [20]. The fine zirconia dispersion in ceramic matrix affects the sinterability [21,22].

TiO_2 addition into cordierite matrix lowered the sintering temperature (1300 ℃). It exhibited better mechanical properties and low coefficient of thermal expansion [23]. A remarkable influence on crystallization was observed with TiO_2 addition for the sintering process carried out using hot-pressing techniques. It reported high strengths for low volume fractions of the reinforced phase (around 10%) [24]. The use of TiO_2 as a nucleating agent for magnesium aluminum silicate (MAS) glass ceramics heat treated at 1100 ℃ for 2 h reported the maximum elastic modulus accompanied by good mechanical properties [25–27].

Cordierite–ceria fabricated by colloidal and sol–gel method showed good results of characterization, with high strength and low thermal expansion [28]. Through investigation, cordierite ceramic containing Ce^{4+} showed the behavior of glass crystallization in $MgO–Al_2O_3–SiO_2–CeO_2$ system. This reduced the temperature of glass softening and delayed the crystallization of μ-cordierite. A small amount of ceria addition dissolved little into cordierite and did not react with cordierite. But it existed as a secondary phase in the ceramic with no reduction in sintering temperature [29]. Reduction in sintering temperature was observed in cordierite processed by powder metallurgy technique [30]. The cordierite ceramic synthesized by co-precipitation technique inhibited the μ-cordierite crystallization and improved α-cordierite crystallization. The 3.2 wt% of Ce^{4+} enhanced the density and mechanical strength [31]. Investigations on the influence of CeO_2 on cordierite's properties showed no remarkable modifications in the microstructure [32]. The results suggested that ceria addition into cordierite presented excellent characteristics as a flux for the sintering of ceramics. This reduced the sintering temperature with enhanced properties. Above literatures show that there has been no extensive study on the thermo-mechanical properties for ceria doped ceramics. The research on development of new materials with good mechanical properties rekindles the research on ceria doped cordierite, due to cordierite's applications in automotive, aerospace, furniture kiln and electrical insulators.

With an objective to study the sintering characteristics and improvement in mechanical properties, cordierite has been taken as a material of study by the addition of ceria (dopant). Since ceria is a highly active substance, it acts as an effective flux in sintering of ceramics. This research was carried out to investigate the synthesis and characterization of cordierite and cordierite doped by the addition of ceria (5–20 wt%) using conventional technique. Characterization such as X-ray diffraction (XRD),

thermogravimetric (TG) and differential thermal analysis (DTA), Fourier transform infrared (FTIR) and scanning electron microscopy (SEM) and the thermo-mechanical properties of cordierite–CeO_2 were investigated.

2 Experimental

2. 1 Sample preparation

In order to synthesize cordierite and cordierite–ceria composite, the raw materials used were pure alumina (99% purity, 5 μm, Aldrich), magnesia (99.95% purity, Aldrich), silica (99.74% purity, < 5 μm, Aashirwad) cerium oxide (99.9% purity, < 5 μm, Aldrich). The pure cordierite powders of stoichiometric composition (MgO 13.8 wt%, Al_2O_3 34.8 wt% and SiO_2 51.4 wt%) were mixed thoroughly, and the ceria doped cordierite powders were prepared with different compositions (5 wt%, 10 wt%, 15 wt% and 20 wt%). The specimens herein were referred as CCZr0, CCe05, CCe10, CCe15 and CCe20 for the noted dopant additions, respectively. The mixed raw powders were wet milled with isopropanol for 3 h, dried at 100 ℃ for 12 h, then followed by dry milling for 2 h to obtain better homogeneity, and added with 1 wt% flux (ethylene glycol) and binder (polyvinyl alcohol) each. The green body samples were compacted at 240 MPa into pellets of 10 mm in diameter. The samples were calcined at 400 ℃ for 3 h to dry out the volatiles. The green body compacts were sintered at different temperatures ranging from 600 ℃ to 1350 ℃ for 3 h at a heating rate of 10 ℃/min.

2. 2 Characterization

The phase transformation and physical behavior at different sintering temperatures were evaluated for the samples synthesized. The phase characterization was done by using XRD (SEIFERT Diffractometer with Cu Kα radiation), FTIR spectrum analysis (Bruker IFS 66V Spectrometer) and TG/DTA (Perkin Elmer simultaneous thermal analyzer) which was carried out at a constant heating rate of 10 ℃/min. The sintered samples were then polished using different grades of polishing sheets and thermally etched at 1200 ℃ for 30 min and SEM micrograph was obtained. The density measurements were then carried out by using the Archimedes principle.

For hardness measurements, sintered samples were grinded and polished with different grades of polishing papers. Indentation hardness testing was performed for a standard load 98.1 N using Vickers hardness tester (Zwick, 3212). The Vickers hardness, H_V, is calculated using the formula:

$$H_V = 1.854 \cdot P/d^2$$

where P is the indentation load (N); d is the mean diagonal (m).

Using indentation fracture method, fracture toughness was evaluated. Fracture toughness (K_{IC}) of the ceramics was estimated for a load (98.1 N), considering 15 s as holding time using the following formula with a Vickers indenter:

$$K_{IC} = 0.319 \cdot P/(al^2)$$

where P is the indentation load (N); c is the crack length (m); a is the half length of the diagonal (m); and $l = c - a$, as described in Fig. 1.

The flexural strength measurement was carried out under three-point bending in a universal testing machine (Shimadzu), considering the cross head speed of 0.5 mm/min. Three specimens in each composition were used with a span length of 25 mm to measure the flexural strength. Thermo-mechanical analysis was conducted to measure the coefficient of thermal expansion with a dilatometer (VB model: from 70 ℃ to 800 ℃ at a heating rate of 10 ℃/min).

3 Results and discussion

3. 1 Characterization studies

Table 1 presents the phase identification of XRD patterns. XRD pattern at 600 ℃ exhibits the amorphous nature of the cordierite and cordierite–ceria samples. Figures 2 and 3 show the progressive phase changes of the pure cordierite sample (CCZr0) and cordierite–ceria (CCe20) heat treated between 600 ℃ and 1350 ℃ for 3 h, respectively.

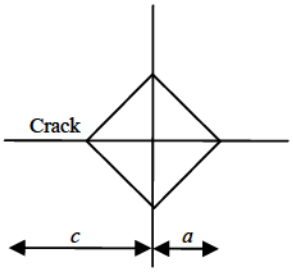

Fig. 1 Fracture toughness measurement procedure representation.

Table 1 Summary of results of XRD studies for pure cordierite and cordierite–ceria

Sample	Phase composition				
	600 ℃	800 ℃	1000 ℃	1200 ℃	1350 ℃
CCZr0	A	MAS	μ, S, C	μ, α, S, C	α, C
CCe05	A	MAS	μ, S, C, Ce	μ, α, S, C, Ce	α, C
CCe10	A	MAS	μ, S, C, Ce	μ, α, S, C, Ce	α, Ce
CCe15	A	MAS	μ, S, C, Ce	μ, α, S, C, Ce	α, Ce
CCe20	A	MAS	μ, S, C, Ce	μ, α, S, C, Ce	α, Ce

A: amorphous; MAS: magnesium aluminum silicate; μ: cordierite (metastable); S: spinel; C: cristobalite; Ce: ceria; α: cordierite (stable).

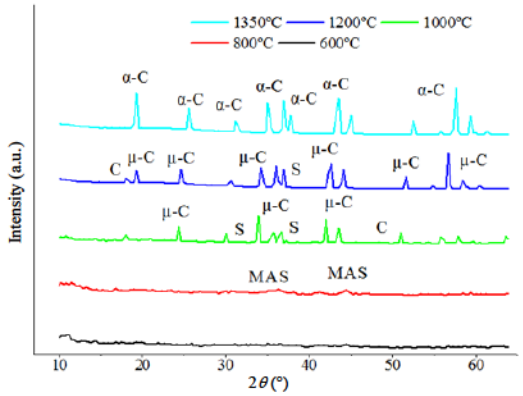

Fig. 2 XRD patterns for pure cordierite powder sample (CCZr0) sintered at different temperatures.

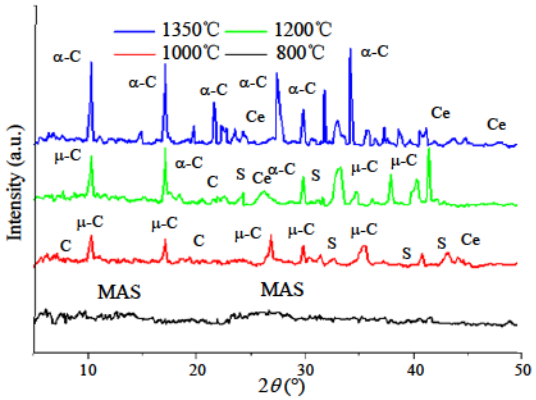

Fig. 3 XRD patterns for cordierite–ceria powder sample (CCe20) sintered at different temperatures.

The presence of magnesium aluminium silicate is observed at 800 ℃ in all samples, and the results obtained were compared with FTIR interpretation at 800 ℃. Vibrations of Al–O or Mg–O occur at 680 cm^{-1} and 734 cm^{-1}, respectively, and 1020 cm^{-1} corresponds to the AlO_4 tetrahedra. The other bands between 1180 cm^{-1} and 1260 cm^{-1} correspond to the presence of SiO_4. For the samples sintered at 1000 ℃ for 3 h, the XRD results confirm the crystallization of the stuffed β-quartz as a major phase with the presence of the spinel phase. The above results obtained are clearly supported by the DTA curve for pure cordierite and cordierite–ceria samples (Figs. 4 and 5) at 934 ℃ and 989 ℃, respectively. It shows the formation of the solid solution of MgO and Al_2O_3 into SiO_2. This indicates that the solid solution of SiO_2 turns into cordierite [29], which is referred as stuffed β-quartz (low temperature metastable μ-cordierite). At 1000 ℃, cristobalite, spinel, μ-cordierite and ceria are observed as crystal phases in samples CCe05–CCe20. The samples at 1200 ℃ reveal that the μ-cordierite starts converting into a high temperature stable structure α-cordierite. The crystalline phases identified in the samples are cristobalite, spinel, μ-cordierite, α-cordierite and ceria. The bands at 1270 cm^{-1}, 1240 cm^{-1}, 1090 cm^{-1}, 720–910 cm^{-1} and 590 cm^{-1} display the presence of μ-cordierite and α-cordierite from the FTIR spectrum (Fig. 6). These results confirm that the cordierite synthesis occurs at sintering temperature above 1200 ℃. At the final sintering temperature (1350 ℃), α-cordierite is formed. The complete crystallization of α-cordierite is due to the disappearance of spinel, μ-cordierite and stuffed β-quartz. The spinel, being a product containing MgO and Al_2O_3, reacts with SiO_2 at high temperatures. The

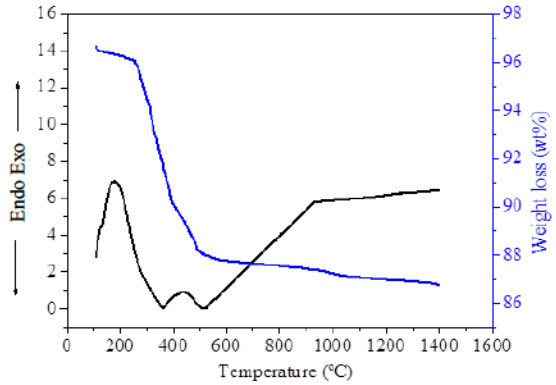

Fig. 4 TG/DTA curve for pure cordierite.

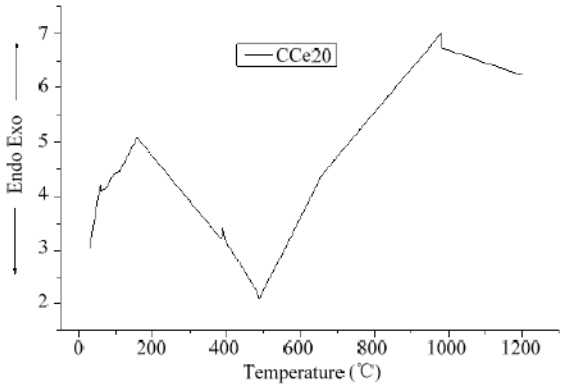

Fig. 5 TG/DTA curve for cordierite–ceria.

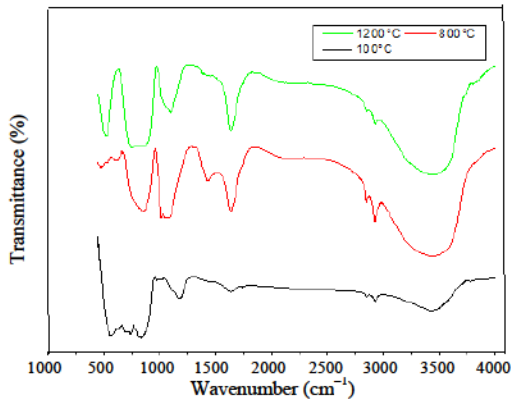

Fig. 6 FTIR spectra of cordierite–ceria sample (CCe20) at different sintering temperatures.

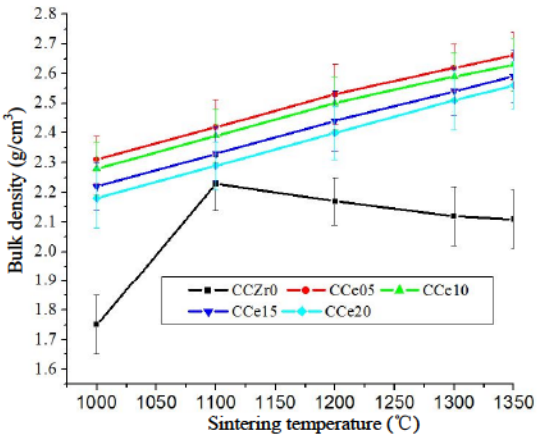

Fig. 7 Bulk density of pure cordierite and cordierite–ceria samples (CCe05–CCe20) at different sintering temperatures.

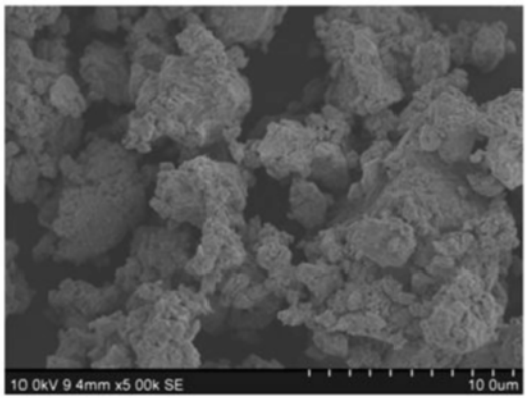

Fig. 8 SEM photograph of pure cordierite specimen sintered at 1350 ℃ for 3 h.

stuffed β-quartz completely reacts with μ-cordierite and transforms into stable α-cordierite. The observation reports that minor amounts of spinel and cristobalite are still present. From the XRD patterns of samples CCe05–CCe20, the ceria addition into the cordierite matrix confirms that it does not form any reaction products. At 1350 ℃, the presence of ceria as a separate phase is observed [28]. The reason for the formation of cordierite at the temperature (1350 ℃) below its sintering temperature (1450 ℃) is due to the fact that the ceria modifies the amorphous to cordierite transformation temperature. Since, Al^{3+}, Mg^{2+} and Si^{4+} in the oxides grow towards the nucleus. By solid-state diffusion process, the crystallization of cordierite occurs [33]. It is found that samples containing Ce^{4+} are composed of cordierite and ceria (Fig. 3). The variation in the peaks observed is due to the ceria additions; this gives the clear correlation that the solubility of ceria is very limited due to the presence of the ceria in the XRD patterns.

3. 2 Microstructural characterization

The bulk density of the cordierite compacts prepared was densified rapidly between 1000 ℃ and 1100 ℃ (Fig. 7). The crystallization of spinel occurs because of the intimately mixed Al^{3+} and Mg^{2+} ions; densification is observed due to formation of some viscous liquid within a very short temperature range. The curve indicates that the densification of cordierite powders stops at the onset of the crystallization of μ-cordierite. The above result is well supported by the study of SEM for cordierite (Fig. 8), which reveals the different sizes of the particles. The densification starts by liquid phase sintering or a viscous flow mechanism prior to crystallization. It is interesting to note that, initially cordierite grain does not change its size and the corners remain sharp, indicating little dissolution and precipitation that take place during densification. But the cordierite–ceria (5–20 wt%) demonstrates that the density increases with an increase in the sintering temperature. The sample CCe05 exhibits the highest density than others. The cordierite–ceria (5 wt%) composite shows a high density due to the decreased softening temperature and strengthened viscous flow [31]. The present study reveals that the addition of CeO_2 into cordierite above 5 wt% leads to higher softening temperatures, prior to viscous flow of amorphous phase [28].

Ceria, known for its softening at earlier temperatures, results in viscous flow filling into the space between the oxide particles. The reason for low densification is that cordierite with addition of higher amounts of ceria (10–20 wt%) has higher softening temperature, prior to the viscous flow of amorphous phases, with CeO_2 precipitation. It should be noted that in order to obtain

denser products, the sintering of the compacts must precede crystallization. The reverse would greatly decrease the mobility of the ions and impede sinterability. The above results are in agreement with the results of bulk density. Figure 9 shows the presence of ceria. The micrograph for cordierite reveals the different sizes of the particles. Densification begins by liquid phase sintering or a viscous flow mechanism prior to crystallization. It is interesting to note that, the initial cordierite grain does not change its size and the corners remain sharp, indicating that little dissolution and precipitation take place during densification.

3. 3 Mechanical testing

Figure 10 shows the Vickers hardness of pure cordierite sample (CCZr0) and cordierite–ceria samples (CCe05–CCe20) for an applied load (10 kgf) as a function of sintering temperature. The hardness of pure cordierite sample (CCZr0) shows an increase in hardness up to 1100 ℃. This could be due to the formation of α-cordierite and spinel phases. Hardness is found to decrease with sintering temperatures above

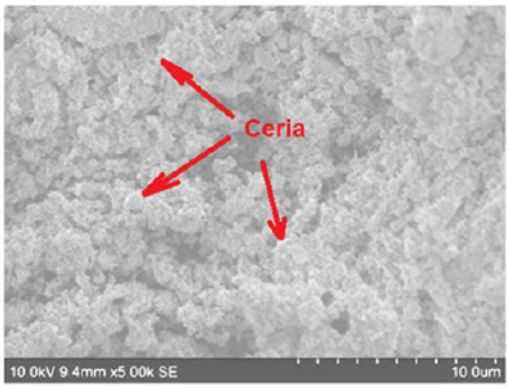

(a)

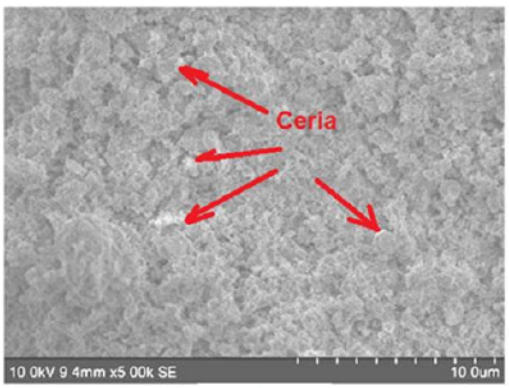

(b)

Fig. 9 SEM photographs of cordierite–ceria specimen sintered at 1350 ℃ for 3 h.

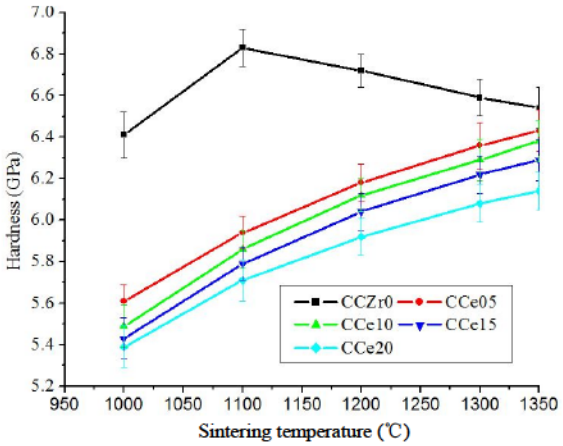

Fig. 10 Vickers hardness of pure cordierite and cordierite–ceria samples (CCe05–CCe20) at different sintering temperatures.

1100 ℃. Vickers hardness of pure cordierite ceramic is found to be 6.54 GPa at the sintering temperature 1350 ℃. In all samples, the hardness shows an increase up to 1350 ℃. Vickers hardness of cordierite–ceria sample (CCe05) sintered at 1350 ℃ was 6.43 GPa. From the observation, sample CCe05 shows a better hardness. The XRD results indicate that in all the samples, ceria transforms the amorphous cordierite to crystallite form, which reduces the formation temperature. This shows the formation of α-cordierite and spinel phases at 1200 ℃. Sample CCe05 exhibits the highest hardness. An increase in ceria content (10–20 wt%) shows decreased hardness, and the characterization studies show that the ceria inclusion does not show any secondary phase. An increased content (10–20 wt%) of CeO_2 in the cordierite matrix dissolves to certain extent. But excess ceria exists as a separate phase along with the cordierite phase. Hence, presence of ceria as a separate phase decreases the hardness of cordierite.

Fracture toughness of pure cordierite (CCZr0) and cordierite–ceria samples (CCe05–CCe20) heat treated at different sintering temperatures is shown in Fig. 11. It is found that the fracture toughness of pure cordierite material is low at 1000 ℃. At 1100 ℃, there is an increase in the fracture toughness. This may be due to the formation of α-cordierite. With the increase in sintering temperatures, fracture toughness decreases due to grain growth. Fracture toughness of pure cordierite at 1350 ℃ is 2.76 $MPa{\cdot}m^{1/2}$. This is due to the fact that an increase in temperature causes anisotropic effects due to thermal expansion in the cordierite crystal. They cause expansion and

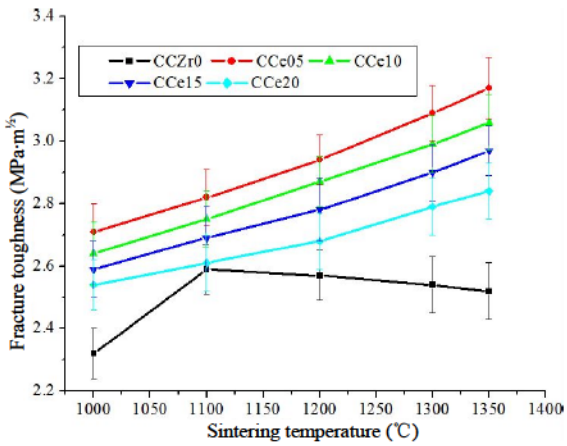

Fig. 11 Fracture toughness of pure cordierite and cordierite–ceria samples (CCe05–CCe20) at different sintering temperatures.

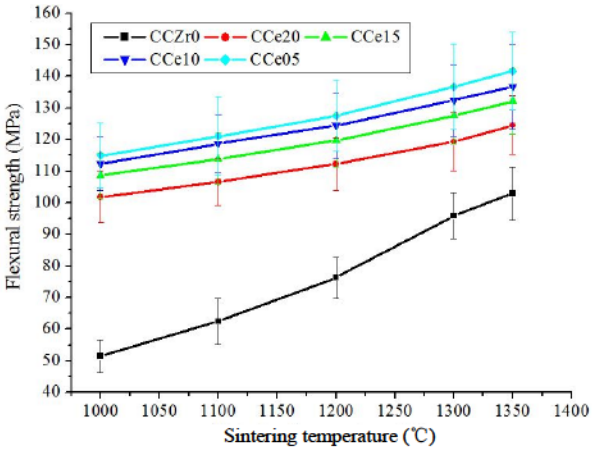

Fig. 12 Flexural strength of pure cordierite and cordierite–ceria samples (CCe05–CCe20) at different sintering temperatures.

contraction, which result in the development of micro cracks and residual stresses. This in turn affects the fracture behavior of the polycrystalline materials. Fracture toughness of cordierite–ceria (CCe05) composite increases with an increase in the sintering temperature, but decreases with the addition of ceria (10–20 wt%) composition up to the maximum sintering temperature of 1350 ℃. Fracture toughness calculated of sample CCe05 is 3.17 MPa·m^{½} at 1350 ℃ for 3 h, which is higher than those of the other samples.

The flexural strength obtained for the pure cordierite and cordierite–ceria samples (CCe05–CCe20) heat treated at various sintering temperatures is shown in Fig. 12. From the results, it is clear that the flexural strength of pure cordierite increases from 51.37 MPa to 102.94 MPa. It increases with increasing sintering temperature, which may be due to the α-cordierite formation. Bulk density results reveal that the porous nature of the samples is responsible for lower flexural strength. Flexural strength of cordierite–ceria (CCe05) increases with an increase in the sintering temperature, which is higher than those of the other compositions of ceria (10–20 wt%). Measured flexural strength of cordierite–ceria (CCe05) is 141.62 MPa. With the increase in sintering temperature, it favors the formation of α-cordierite. Flexural strength is found to increase in all the samples up to 1350 ℃. Results prove that the flexural strength of cordierite is enhanced due to the dispersion of ceria in the cordierite matrix. Finally, the studies show that the addition of ceria by 5 wt% confirms the increase in flexural strength.

3.4 Thermal properties

Thermal expansion studies were performed for pure cordierite (CCZr0) and cordierite–ceria (CCe05) sintered at 1350 ℃. CTE was measured using a dilatometer in the temperature range of 70 ℃ to 800 ℃. The samples pure cordierite (CCZr0) and cordierite–ceria (CCe05) record 4.54×10^{-6} $(℃)^{-1}$ and 3.86×10^{-6} $(℃)^{-1}$ at 800 ℃, respectively. Principal reason for the difference in values of CTE of pure cordierite with standard value is due to the presence of particles like α-alumina and cristobalite with large CTE which is confirmed from the XRD results. However, the sample CCe05 shows low value of CTE, which confirms the formation of α-cordierite as the major phase. It is clear that ceria has a higher CTE (6.0×10^{-6} $(℃)^{-1}$) compared to pure cordierite (1.7×10^{-6} $(℃)^{-1}$). The observed low coefficient of thermal expansion is due to the combined effects of the cerium absorption, thermal treatment and solubility of ceria in cordierite phase.

4 Conclusions

Pure cordierite and ceria doped cordierite composites were successfully synthesized by conventional process. The results of thermo-mechanical studies revealed high hardness, fracture toughness and flexural strength for cordierite mixed with ceria by 5 wt%. The thermogravimetric analysis showed the weight loss and the differential thermal analysis curve showed the formation and transformation of the crystalline phases. The crystallization of the different phases was

confirmed for the samples heat treated at different temperatures by the X-ray diffraction studies. The pure cordierite and ceria doped cordierite by 5 wt% powders showed cordierite as a single phase, and the other compositions with the presence of cordierite and ceria as a secondary phase. The Fourier transform infrared spectra revealed the functional groups and ordering of the polymorphic-transition of ceria doped cordierite composites for different heat treated samples. Sintered samples exhibited a dense and homogeneous mixture, by the uniform spatial distribution of ceria particles throughout the matrix. Cordierite–ceria (5 wt%) exhibited better mechanical properties than other cordierite–ceria samples (10–20 wt%). The results of cordierite–ceria (5 wt%) obtained were as follows: hardness of 6.43 GPa, fracture toughness of 3.17 $MPa \cdot m^{½}$, flexural strength of 141.63 MPa and low coefficient of thermal expansion 3.86×10^{-6} $(℃)^{-1}$ at 800 ℃. Hardness of cordierite–ceria ceramic did influence cordierite ceramic composite at higher sintering temperature through secondary phase formation in comparison with cordierite. Better mechanical properties of cordierite–ceria confirmed the suitability as an alternate material for cordierite.

Acknowledgements

The authors would like to thank the Department of Mechanical Engineering, Anna University, Chennai, and SMBS, VIT University Chennai, India for providing the facilities to carry out this research work.

References

[1] Trumbulovic Lj, Acimovic Z, Panic S, *et al*. Synthesis and characterization of cordierite from kaolin and talc for casting application. *FME Transactions* 2003, **31**: 43–47

[2] Rankin GA, Mervin HE. Ternary system $MgO–Al_2O_3–SiO_2$. *J Am Ceram Soc* 1918, **45**: 301–325.

[3] Gibbs GV. The polymorphism of cordierite I: The crystal structure of low cordierite. *Am Mineral* 1966, **51**: 1068–1087.

[4] Chahal LE, Werckmann J, Pourroy G, *et al*. X-ray and electron diffraction studies on crystallization of two cordierite precursors prepared by atomization or sol–gel process. *J Cryst Growth* 1995, **156**: 99–107.

[5] Kazakos AM, Komarneni S, Roy R. Sol–gel processing of cordierite: Effect of seeding and optimization of heat treatment. *J Mater Res* 1990, **5**: 1095–1103.

[6] Jean J-H, Gupta TK. Liquid-phase sintering in the glass–cordierite system. *J Mater Sci* 1992, **27**: 1575–1584.

[7] Knickerbocker SH, Kumar AH, Herron LW. Cordierite glass–ceramics for multilayer ceramic packaging. *Am Ceram Soc Bull* 1993, **72**: 90–95.

[8] Sumi K, Koyabashi Y, Kato E. Low-temperature fabrication of cordierite ceramics from kaolinite and magnesium hydroxide mixtures with boron oxide additions. *J Am Ceram Soc* 1999, **82**: 783–785.

[9] Parmelee GW, Baldwin GH. Anvendung von Talk in Porzellanmassen. *Trans Amer Soc* 1913, **15**: 606–615.

[10] Parmelee GW, Thurnauer H. Some effects of additions to a talk body. *Bull Am Ceram Soc* 1935, **14**: 69.

[11] Camerucci MA, Urretavizcaya G, Cavalieri AL. Sintering of cordierite based materials. *Ceram Int* 2003, **29**: 159–168.

[12] Oliveira FAC, Fernandes JC. Mechanical and thermal behaviour of cordierite–zirconia composites. *Ceram Int* 2002, **28**: 79–91.

[13] Thorp JS, Hutton W. Radiation induced paramagnetic centres in $MgO–Al_2O_3–SiO_2$ glasses containing TiO_2. *J Phys Chem Solids* 1981, **42**: 843–855.

[14] Yalamaç E, Akkurt S. Additive and intensive grinding effects on the synthesis of cordierite. *Ceram Int* 2006, **32**: 825–832.

[15] Ozel E, Kurama S. Effect of the processing on the production of cordierite–mullite composite. *Ceram Int* 2010, **36**: 1033–1039.

[16] Claussen N. Fracture toughness of Al_2O_3 with an unstabilized ZrO_2 dispersed phase. *J Am Ceram Soc* 1976, **59**: 49–51.

[17] Claussen, N. Stress-induced transformation of tetragonal ZrO_2 particles in ceramic matrices. *J Am Ceram Soc* 1978, **61**: 85–86.

[18] Evans AG, Heuer AH. Review—Transformation toughening in ceramics: Martensitic transformations in crack-tip stress fields. *J Am Ceram Soc* 1980, **63**: 241–248.

[19] Hannink RHJ, Kelly PM, Muddle BC. Transformation toughening in zirconia-containing ceramics. *J Am Ceram Soc* 2000, **83**: 461–487.

[20] Hirvonen A, Nowak R, Yamamoto Y, *et al*. Fabrication, structure, mechanical and thermal properties of zirconia-based ceramic nanocomposites. *J Eur Ceram Soc* 2006, **26**: 1497–1505.

[21] Sun E-H, Choa Y-H, Sekino T, *et al*. Pressureless sintering and characterization of cordierite/ZrO_2 composites. *Mater Res Innov* 2002, **6**: 105–111.

[22] Gusev AA, Avvakumov EG, Virokurova OB, *et al*. The effect of transition metal oxides on the strength, phase composition, and microstructure of cordierite ceramics. *Glass Ceram*+ 2001, **58**: 24–26.

[23] Senthil Kumar M, Elaya Perumal A. Synthesis, characterization and sintering behaviour influencing mechanical, thermal and physical properties of cordierite-doped TiO_2. *J Mater Res Technol* 2013, **2**: 269–275.

[24] Piñero M, Zarzycki J. Processing of ZrO_2 reinforced cordierite composites by infiltration of ceramic felt with sonosols. *J Sol–Gel Sci Technol* 1994, **1**: 275–283.

[25] Shao H, Liang K, Peng F. Crystallization kinetics of $MgO–Al_2O_3–SiO_2$ glass–ceramics. *Ceram Int* 2004, **30**: 927–930.

[26] Wange P, Höche T, Rüssel C, *et al*. Microstructure–property relationship in high-strength $MgO–Al_2O_3–SiO_2–TiO_2$ glass–ceramics. *J Non-Cryst Solids* 2002, **298**: 137–145.

[27] Weaver DT, Van Aken DC, Smith JD. The role of TiO_2 and composition in the devitrification of near-stoichiometric cordierite. *J Mater Sci* 2004, **39**: 51–59.

[28] Shi ZM, Liu Y, Yang WY, *et al*. Evaluation of cordierite–ceria composite ceramics with oxygen storage capacity. *J Eur Ceram Soc* 2002, **22**: 1251–1256.

[29] Shi ZM, Liang KM, Gu SR. Effects of CeO_2 on phase transformation towards cordierite in $MgO–Al_2O_3–SiO_2$ system. *Mater Lett* 2001, **51**: 68–72.

[30] Galakhov AV, Shevchenko V, Stebunov AA. Phase inversions in Al–Si–Mg gels. Influence of Ti, Ce, and Zr additions. *Refractories* 1991, **32**: 286–289.

[31] Kim BH, Lee KH. Crystallization and sinterability of cordierite-based glass powders containing CeO_2. *J Mater Sci* 1994, **29**: 6592–6598.

[32] Montorsi MA, Delorenzo R, Verné E. Cordierite–cerium (IV) oxide system: Microstructure and properties. *Ceram Int* 1994, **20**: 353–358.

[33] Shi ZM, Bai X, Wang XF. Ce^{4+}-modified cordierite ceramics. *Ceram Int* 2006, **32**: 723–726.